Journal of the Egyptian Mathematical Society (2015) 23, 445–450

Egyptian Mathematical Society

Journal of the Egyptian Mathematical Society

www.etms-eg.org
www.elsevier.com/locate/joems

ORIGINAL ARTICLE

Heat transfer analysis for squeezing flow between parallel disks

Sheikh Irfanullah Khan [a,b], Naveed Ahmed [b], Umar Khan [b], Saeed Ullah Jan [a], S.T. Mohyud-Din [b,*]

[a] *COMSATS Institute of Information Technology, University Road, Abbottabad, Pakistan*
[b] *Department of Mathematics, Faculty of Sciences, HITEC University, Taxila Cantt, Pakistan*

Received 20 August 2013; accepted 18 June 2014
Available online 18 March 2015

KEYWORDS

Squeezing flow;
Magnetic field;
Variational iteration method (VIM);
Parallel disks

Abstract Heat transfer analysis for the squeezing magneto-hydrodynamic (MHD) flow of a viscous incompressible fluid between parallel disks is considered. Upper disk is movable in upward and downward directions while the lower disk is fixed but permeable. Viable similarity transforms are used to convert the conservation law equations to a system of nonlinear ordinary differential equations. Resulting system is solved by using variational iteration method (VIM). Influence of flow parameters is discussed and numerical solution is sought using RK-4 method. A convergent solution is obtained just after few numbers of iterations.

MATHEMATICS SUBJECT CLASSIFICATION: 35Q79; 76D05; 76M55

© 2014 Production and hosting by Elsevier B.V. on behalf of Egyptian Mathematical Society.

1. Introduction

Heat transfer in rapidly moving engines and machines with lubricants inside has been an active field of research. For safe and consistent working of such machines it is necessary to study heat transfer in these systems. Several attempts are reported in this regard after the pioneer work done by Stefan [1]. Two-dimensional MHD squeezing flow between parallel plates has been examined by Siddiqui et al. [2]. For parallel disk similar problem has been discussed by Domairy and Aziz [3]. Both used homotopy perturbation method (HPM) to determine the solution.

Joneidi et al. [4] studied the mass transfer effect on squeezing flow between parallel disks using homotopy analysis method (HAM). Most recently, influence of heat transfer in the MHD squeezing Flow between parallel disks has been investigated by Hayat et al. [5]. They used HAM to solve the resulting nonlinear system of ordinary differential equations.

Motivated by the preceding work here we present heat transfer analysis for the MHD squeezing flow between parallel disks. Well known variational iteration method (VIM) [7–11] has been employed to solve system of highly nonlinear differential equations that govern the flow. VIM is a strong

* Corresponding author at: Department of Mathematics, Faculty of Sciences, HITEC University, Taxila Cantt, Pakistan.
E-mail address: syedtauseefs@hotmail.com (S.T. Mohyud-Din).

Peer review under responsibility of Egyptian Mathematical Society.

Production and hosting by Elsevier

http://dx.doi.org/10.1016/j.joems.2014.06.011
1110-256X © 2014 Production and hosting by Elsevier B.V. on behalf of Egyptian Mathematical Society.

analytical technique and has been employed by several researchers in recent times to study different type of problems [12–21]. The main positive features of this technique is its simplicity, selection of initial approximation, compatibility with the nonlinearity of physical problems of diversified complex nature, minimal application of integral operator and rapid convergence [21].

Numerical solution is also sought to check the validity of analytical solution. A detailed comparison between purely analytical solution obtained by VIM and the numerical solution obtained by employing RK-4 method is presented. It is evident from this article that the VIM provides excellent results with less amount of laborious computational work.

2. Mathematical formulation

MHD flow of a viscous incompressible fluid is taken into consideration through a system consisting of two parallel infinite disks distance $h(t) = H(1-at)^{1/2}$ apart. Magnetic field proportional to $B_0(1-at)^{1/2}$ is applied normal to the disks. It is assumed that there is no induced magnetic field. T_w and T_h represent the constant temperatures at $z = 0$ and $z = h(t)$ respectively. Upper disk at $z = h(t)$ is moving with velocity $\frac{aH(1-at)^{-1/2}}{2}$ toward or away from the static lower but permeable disk at $z = 0$ as shown in Fig. 1. We have chosen the cylindrical coordinates system (r, ϕ, z). Rotational symmetry of the flow $(\partial/\partial\phi = 0)$ allows us to take azimuthal component v of the velocity $V = (u, v, w)$ equal to zero. As a result, the governing equation for unsteady two-dimensional flow and heat transfer of a viscous fluid can be written as [6]

$$\frac{\partial u}{\partial r} + \frac{u}{r} + \frac{\partial w}{\partial z} = 0, \tag{1}$$

$$\rho\left(\frac{\partial u}{\partial t} + u\frac{\partial u}{\partial r} + w\frac{\partial u}{\partial z}\right) = -\frac{\partial \hat{p}}{\partial r} + \mu\left(\frac{\partial^2 u}{\partial r^2} + \frac{\partial^2 u}{\partial z^2} + \frac{1}{r}\frac{\partial u}{\partial r} - \frac{u}{r^2}\right) - \frac{\sigma}{\rho}B^2(t)u, \tag{2}$$

$$\rho\left(\frac{\partial w}{\partial t} + u\frac{\partial w}{\partial r} + w\frac{\partial w}{\partial z}\right) = -\frac{\partial \hat{p}}{\partial z} + \mu\left(\frac{\partial^2 w}{\partial r^2} + \frac{\partial^2 w}{\partial z^2} + \frac{1}{r}\frac{\partial w}{\partial r}\right), \tag{3}$$

$$C_p\left(\frac{\partial T}{\partial t} + u\frac{\partial T}{\partial r} + w\frac{\partial T}{\partial z}\right) = \frac{K_0}{\rho}\left(\frac{\partial^2 T}{\partial r^2} + \frac{\partial^2 T}{\partial z^2} + \frac{1}{r}\frac{\partial T}{\partial r} - \frac{u}{r^2}\right) + v\left\{2\frac{u^2}{r^2} + \left(\frac{\partial u}{\partial z}\right)^2 + 2\left(\frac{\partial w}{\partial z}\right)^2 + 2\left(\frac{\partial u}{\partial r}\right)^2 + 2\left(\frac{\partial w}{\partial r}\right)^2 + 2\frac{\partial u}{\partial z}\frac{\partial w}{\partial r}\right\}, \tag{4}$$

Auxiliary conditions are [5]

$$u = 0, \quad w = \frac{dh}{dt} \quad \text{at } z = h(t) \qquad u = 0, \quad w = -w_0 \quad \text{at } z = 0. \tag{5}$$

$$T = T_w \quad \text{at } z = 0 \qquad u = T_h \quad \text{at } z = h(t). \tag{6}$$

u and w here are the velocity components in r and z directions respectively, μ is dynamic viscosity, $\hat{p}$ is the pressure and ρ is density. Further T denotes temperature, K_0 is thermal conductivity, C_p is specific heat, v is kinematic viscosity and w_0 is suction/injection velocity.

Using the following transformations [5]

$$u = \frac{ar}{2(1-at)}f'(\eta), \quad w = -\frac{aH}{\sqrt{1-at}}f(\eta), \quad B(t) = \frac{B_0}{\sqrt{1-at}}, \quad \eta = \frac{z}{H\sqrt{1-at}}, \quad \theta = \frac{T - T_h}{T_w - T_h}, \tag{7}$$

into Eqs. (2)–(4) and eliminating pressure terms from the resulting equations, we obtain

$$f'''' - S(\eta f''' + 3f'' - 2ff''') - M^2 f'' = 0, \tag{8}$$

$$\theta'' + S\,\Pr(2f\theta' - \eta\theta') - \Pr\, Ec\left(f''^2 + 12\delta^2 f'^2\right) = 0, \tag{9}$$

with the associated conditions

$$f(0) = A, \quad f'(0) = 0, \quad \theta(0) = 1, \qquad f(1) = \frac{1}{2}, \quad f'(1) = 0, \quad \theta(1) = 0, \tag{10}$$

where S denotes the squeeze number, A is suction/injection parameter, M is Hartman number, Pr Prandtl number, Ec modified Eckert number, and δ denotes the dimensionless length defined as

$$S = \frac{aH^2}{2v}, \quad M^2 = \frac{aB_0^2H^2}{v}, \quad \Pr = \frac{\mu C_p}{K_0}, \quad Ec = \frac{1}{C_p(T_w - T_h)}\left(\frac{ar}{2(1-at)}\right)^2, \quad \delta^2 = \frac{H^2(1-at)}{r^2}. \tag{11}$$

Skin friction coefficient and the Nusselt number are defined in terms of variables (7) as

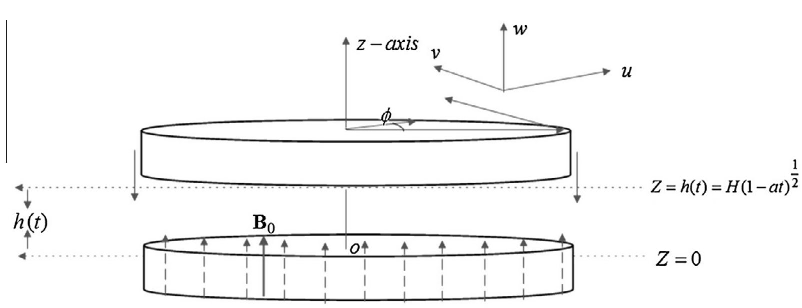

Figure 1 Geometry of the problem.

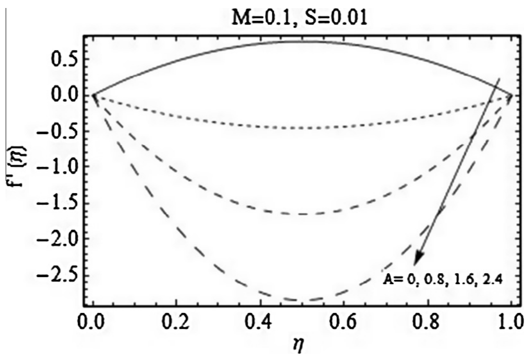

Figure 2 Effect of A on $\theta(\eta)$.

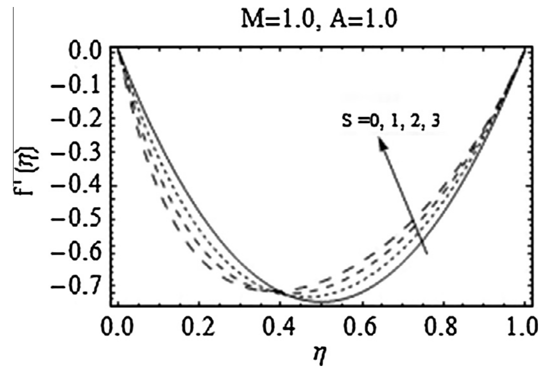

Figure 3 Effect of S on $\theta(\eta)$.

$$\frac{H^2}{r^2} Re_r C_{fr} = f''(1), \quad (1-at)^{1/2} Nu = -\theta'(1), \tag{14}$$

$$Re_r = \frac{raH(1-at)^{1/2}}{2v}. \tag{15}$$

3. Solution scheme

Using proposed procedure for variational iteration method (VIM) [7–21] to solve Eq. (8) and (9) with the associated boundary conditions (10), we have the following iterative schemes

$$f_{n+1}(\eta) = f_n(\eta) - \int_0^\eta \frac{(s-\eta)^3}{3!} \times \begin{pmatrix} f_n^{(4)}(s) - S\left(3f_n''(s) + sf_n'''(s) - 2f_n(s)f_n'''(s)\right) \\ -M^2 f_n(s) f_n''(s) \end{pmatrix} ds, \tag{16}$$

and

$$\theta_{n+1}(\eta) = \theta_n(\eta) - \int_0^\eta (s-\eta)\Big(S\ \mathrm{Pr}\left(2f_n(s)\theta_n'(s) - s\theta_n'(s)\right) + \mathrm{Pr}E\left(\left(f_n''(s)\right)^2 + 12\delta^2\left(f_n'(s)\right)^2\right)\Big) ds, \tag{17}$$

with $n = 0, 1, 2, \ldots$

The first two approximant of the solutions are given by

$$f_0(\eta) = A + \frac{1}{2}A_1\eta^2 + \frac{1}{6}A_2\eta^3, \tag{18}$$

$$\begin{aligned} f_1(\eta) = {} & A + \frac{1}{2}A_1\eta^2 + \frac{1}{6}A_2\eta^3 \\ & + \left(-\frac{1}{12}SAA_2 + \frac{1}{8}SA_1 + \frac{1}{24}M^2A_1\right)\eta^4 \\ & + \left(\frac{1}{30}SA_2 + \frac{1}{120}M^2A_2\right)\eta^5 - \frac{1}{360}SA_1A_2\eta^6 - \frac{1}{2520}SA_2^2\eta^7. \end{aligned} \tag{19}$$

Similarly for (17) we have

$$\theta_0(\eta) = 1 + D\eta, \tag{21}$$

$$\begin{aligned} \theta_1(\eta) = {} & 1 + D\eta + \left(-S\mathrm{Pr}AD - \frac{1}{2}\mathrm{Pr}EcA_1^2\right)\eta^2 \\ & + \left(\frac{1}{6}S\,\mathrm{Pr}D - \frac{1}{3}\mathrm{Pr}EcA_1A_2\right)\eta^3 \\ & + \left(-\frac{1}{2}\mathrm{Pr}EcA_2^2 - \mathrm{Pr}Ec\delta^2A_1^2 - \frac{1}{12}S\,\mathrm{Pr}A_1D\right)\eta^4 \\ & + \left(-\frac{3}{5}\mathrm{Pr}Ec\delta^2A_1A_2 - \frac{1}{60}S\mathrm{Pr}A_2D\right)\eta^5 - \frac{1}{10}\mathrm{Pr}Ec\delta^2A_2^2\eta^6. \end{aligned} \tag{22}$$

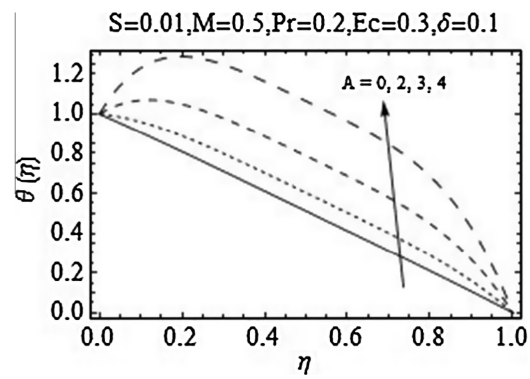

Figure 4 Effect of A on $\theta(\eta)$.

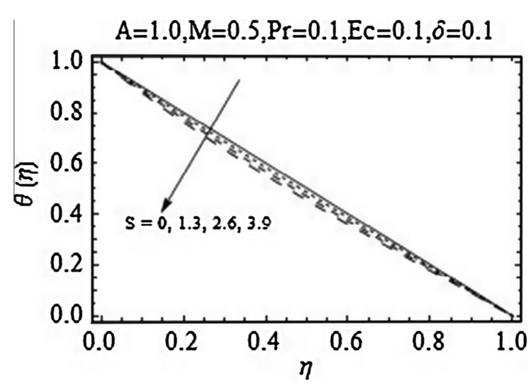

Figure 5 Effect of S on $\theta(\eta)$.

We can find further approximants of the solutions in a similar fashion.

4. Results and discussions

Effects of different flow parameters on the velocity and temperature distributions are discussed in this section for both the suction and injection cases. It is mentionable that after just the three iterations we obtain a convergent solution. After checking the results for several iterations we have verified this convergence. Therefore to show graphical simulation we use third order approximants in coming subsections. Discussions are divided into two subsections; one is for suction case and the other for injection scenario.

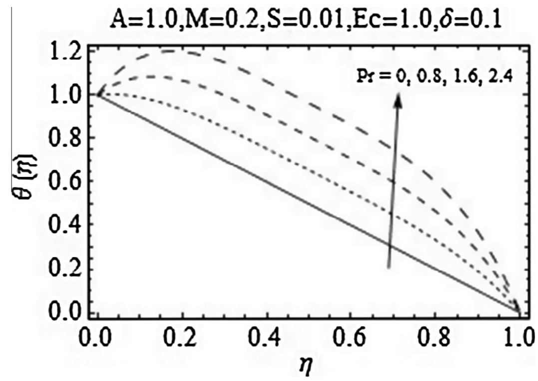

Figure 6 Effect of Pr on $\theta(\eta)$.

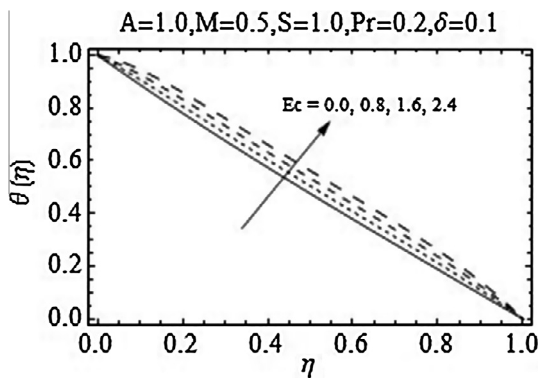

Figure 7 Effect of Ec on $\theta(\eta)$.

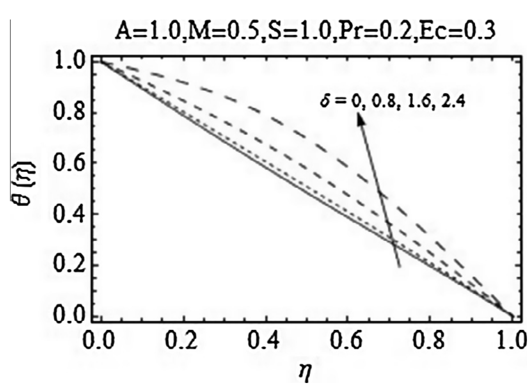

Figure 8 Effect of δ on $\theta(\eta)$.

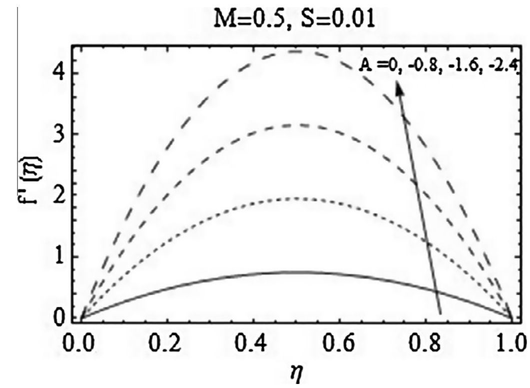

Figure 9 Effect of A on $f'(\eta)$.

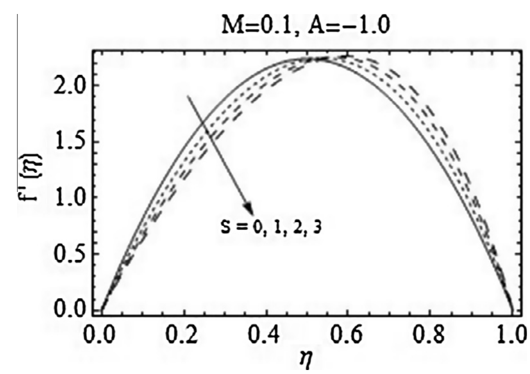

Figure 10 Effect of S on $f'(\eta)$.

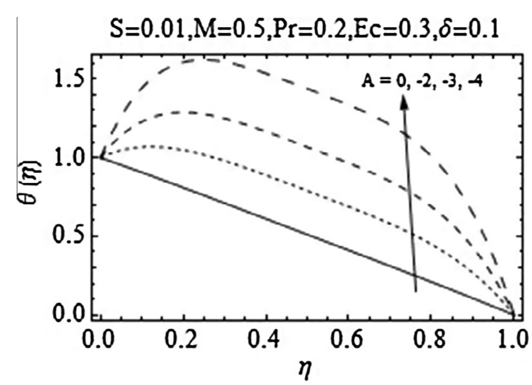

Figure 11 Effect of A on $\theta(\eta)$.

4.1. Suction case ($\boldsymbol{A > 0}$)

Fig. 2 shows the influence of porosity parameter A on the radial and axial velocity. It is clear from Fig. 2(a) that the axial velocity increases with increasing values of A. Boundary layer thickness however is a decreasing function of A. Due to the permeability of upper disk when suction plays a dominant role it allows the fluid to flow near the walls which results in a thinner boundary layer. Effects of deformation parameter S are displayed in Fig. 3. $S > 0$ corresponds to the movement of upper disk away from the lower static disk while $S < 0$ stands for its fall toward the lower disk. It can be seen from Fig. 3 that the absolute of $f'(\eta)$ increases for increasing S in the range of $0 < \eta \leqslant 0.4$, while an opposite behavior in absolute velocity is observed for $0.4 < \eta \leqslant 1$.

To exhibit the effects of flow parameters (in suction case) on the temperature profile Figs. 4–8 are presented. Fig. 4 shows $\theta(\eta)$ to be an increasing function of A, on the other hand thermal boundary layer becomes thinner with raising A. Consequences of increasing S are presented in Fig. 5 according to which temperature profile falls with surging S. Influence of Pr number on the temperature distribution is displayed in Fig. 6 which declares $\theta(\eta)$ to be directly variant with Pr. On the other hand thermal boundary layer is inversely proportional to Pr, it is due to the fact that for higher Pr low

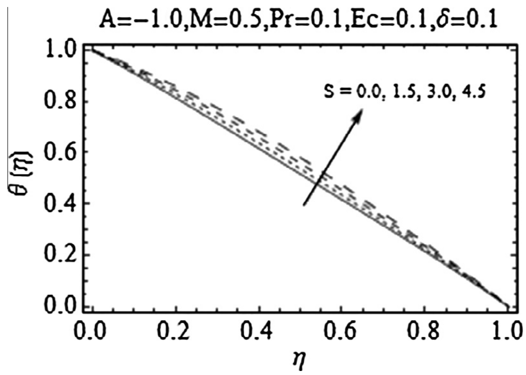

Figure 12 Effect of S on $\theta(\eta)$.

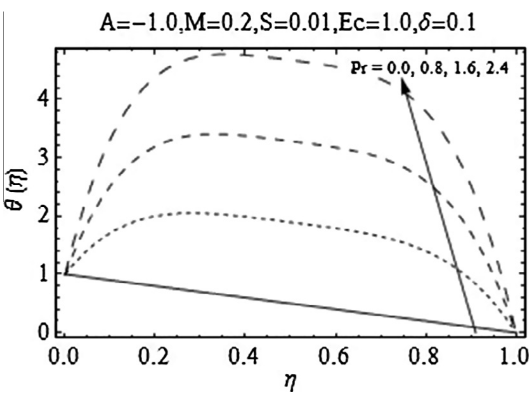

Figure 13 Effect of Pr on $\theta(\eta)$.

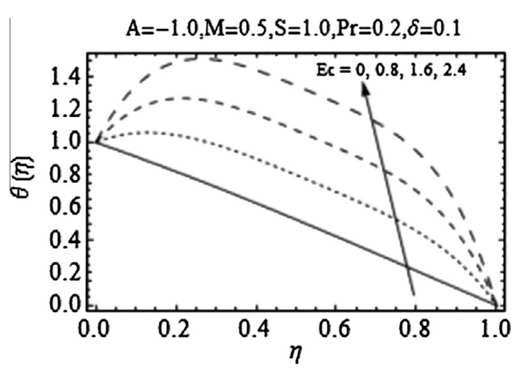

Figure 14 Effect of Ec on $\theta(\eta)$.

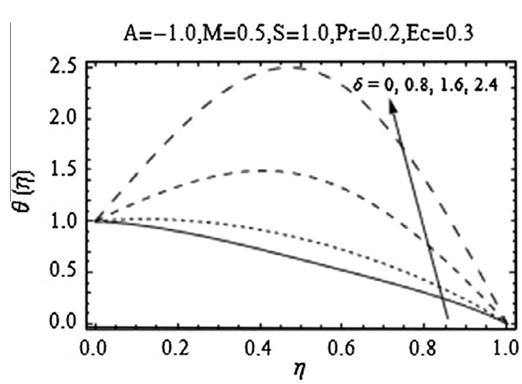

Figure 15 Effect of δ on $\theta(\eta)$.

Table 1 Comparison of numerical and VIM solutions for diverging channel for $\delta = 0.1$, $A = 0.1$, $S = 0.1$, $M = 0.2$, $\Pr = 0.3$ and $Ec = 0.2$.

η	$f'(\eta)$		$\theta(\eta)$	
	VIM	Numerical	VIM	Numerical
0	0	0	1	1
0.2	0.384801	0.384801	0.806144	0.806144
0.4	0.575554	0.575554	0.607022	0.607022
0.6	0.575174	0.575174	0.407004	0.407004
0.8	0.384040	0.384040	0.206121	0.206121
1	0	0	0	0

Table 2 Values of skin friction coefficient $\frac{H^2}{r^2} Re_r C_{fr}$ and the Nusselt number $(1-at)^{1/2}Nu$ for different values of A, S, and M.

A	S	M	$\frac{H^2}{r^2} Re_r C_{fr}$	Pr	Ec	δ	$(1-at)^{1/2}Nu$
−0.1	0.1	0.2	−3.62306	0.3	0.2	0.1	1.1317
0.0			−3.01553				1.0906
0.1			−2.40948				1.0568
0.2			−1.80490				1.0304
0.1	0.01		−2.40239				1.0581
	0.2		−2.41735				1.0553
	0.3		−2.42522				1.0538
	0.1	0.01	−2.40789				1.0568
		0.1	−2.40828				1.0568
		0.2	−2.40948				1.0568

Table 3 Values of Nusselt number $(1-at)^{1/2}Nu$ for different values of Pr, Ec, and δ when $A = 0.1, S = 0.1, M = 0.2$.

Pr	Ec	δ	$(1-at)^{1/2}Nu$
0.0			1.00000
0.1			1.01894
0.2			1.03787
0.3	0.0		0.99860
	0.2		1.05680
	0.4		1.11501
	0.3	0.0	1.08487
		0.5	1.11074
		1.0	1.18836

thermal conductivity is observed which results in narrow thermal boundary layer. Higher values of Prandtl number are associated with large viscosity oils while lowers Pr corresponds to low viscosity fluids. Figs. 7 and 8 indicate that Eckert number Ec and dimensionless length $\theta(\eta)$ have similar effects on temperature profile as Pr.

4.2. Injection case ($A < 0$)

Effects of physical parameters on velocity and temperature distributions for the case of injection are displayed in Figs. 9–15. It is observed that on velocity profiles, effects of involved parameters are opposite to the ones discussed earlier for suction case. Behavior of temperature distribution however remains invariant for both the suction and injection cases.

Further to support our analytical scheme (VIM) we seek a numerical solution using fourth order Runge Kutta method. Table 1 shows a comparison between purely analytical solution obtained by variational iteration method and numerical solution found by RK-4 method. It is evident from the table that both the solutions agree exceptionally well which shows the effectiveness of proposed analytical technique.

Tables 2 and 3 display the numerical values of Nusselt number and coefficient of skin friction for different values of flow parameters. Absolute of skin friction is found to be a decreasing function of permeability parameter A. This observation is important due to its industrial implication since the amount of energy required to squeeze the disk can be reduced by increasing values of A. As discussed earlier the suction parameter A decreases the thermal boundary layer thickness hence at the plates we have higher rate of heat transfer.

4.3. Conclusions

Heat transfer analysis is taken into account for the squeezing flow between parallel disks. VIM is used to determine the series solution to both velocity and temperature distributions. Main upshots of this study are presented as below:

- It is observed that the series solution for velocity converges after third iteration and a convergent solution for temperature profile is obtained just after two iterations.
- Numerical solution obtained by RK-4 method is also compatible with the analytical solution obtained by employing VIM.
- The behavior of all physical parameters is opposite on velocity profile in the cases of suction and injection. On the other hand the effect of parameters remains similar on temperature profile for both suction and injection cases.
- Temperature $\theta(\eta)$ is directly proportional to the Prandtl number.

Acknowledgment

The authors are highly grateful for the valuable comments made by the unknown referees' and editor which really improved the quality of presented work.

References

[1] M.J. Stefan, Versuchs Uber die scheinbare adhesion, Sitzungsberichte der Akademie der Wissenschaften in Wien. Mathematik-Naturwissen 69 (1874) 713–721.

[2] A.M. Siddiqui, S. Irum, A.R. Ansari, Unsteady squeezing flow of a viscous MHD fluid between parallel plates, M. Mod. Ana 13 (2008) 565–576.

[3] G. Domairy, A. Aziz, Approximate analysis of MHD squeeze flow between two parallel disks with suction or injection by homotopy perturbation method, Math. Prob. Eng. (article ID/2009/603916).

[4] A.A. Joneidi, G. Domairry, M. Babaelahi, Effect of mass transfer on the flow in the magnetohydrodynamic squeeze film between two parallel disks with one porous disk, Chem. Eng. Comm. 198 (2011) 299–311.

[5] T. Hayat, A. Yousuf, M. Mustafa, S. Asghar, Influence of heat transfer in the squeezing flow between parallel disks, Chem. Eng. Comm. 199 (2012) 1044–1062.

[6] M. Sajid, I. Ahmad, T. Hayat, M. Ayub, Series solution for unsteady axisym-metric flow and heat transfer over a radially stretching sheet, Comm. Non-Lin. Sci. Num. Simul. 13 (2008) 2193–2202.

[7] J.H. He, Variational iteration method, A kind of nonlinear analytical technique, some examples, Int. J. Nonlin. Mech. 34 (1999) 699–708.

[8] J.H. He, Variational iteration method for autonomous ordinary differential systems, Appl. Math. Comput 114 (2000) 115–123.

[9] J.H. He, An elementary introduction of recently developed asymptotic methods and nanomechanics in textile engineering, Int. J. Mod. Phys. B 22 (21) (2008) 3487–4578.

[10] J.H. He, Some asymptotic methods for strongly nonlinear equation, Int. J. Mod. Phys. B 20 (2006) 1144–1199.

[11] J.H. He, Variational iteration method – some recent results and new interpretations, J. Comp. Appl. Math. 207 (2007) 3–17.

[12] J.H. He, X. Wu, Variational iteration method: new developments and applications, Comp. Math. Appl. 54 (2007) 881–894.

[13] J.H. He, X.H. Wu, Construction of solitary solution and compaction-like solution by variational iteration method, Chaos, Solit. Fract. 29 (1) (2006) 108–113.

[14] M.A. Abdou, A.A. Soliman, Variational iteration method for solving Burger's and coupled Burger's equations, J. Comp. Appl. Math 181 (2005) 245–251.

[15] S. Abbasbandy, Numerical solution of non-linear Klein–Gordon equations by variational iteration method, Int. J. Numer. Meth. Eng. 70 (7) (2007) 876–881.

[16] M.A. Noor, S.T. Mohyud-Din, Variational iteration technique for solving higher order boundary value problems, Appl. Math. Comp. 189 (2007) 1929–1942.

[17] M.A. Noor, S.T. Mohyud-Din, Variational iteration method for solving higher-order nonlinear boundary value problems using He's polynomials, Int. J. Nonlin. Sci. Numer. Sim 9 (2) (2008) 141–157.

[18] S.T. Mohyud-Din, M.A. Noor, K.I. Noor, M.M. Hosseini, Variational iteration method for re-formulated partial differential equations, Int. J. Nonlin. Sci. Numer. Sim 11 (2) (2010) 87–92.

[19] S.T. Mohyud-Din, M.A. Noor, K.I. Noor, M.M. Hosseini, Solution of singular equations by He's variational iteration method, Int. J. Nonlin. Sci. Numer. Sim 11 (2) (2010) 81–86.

[20] S.T. Mohyud-Din, U. Khan, N. Ahmed, Z.A. Zaidi, S.I.U. Khan, X.J. Yung, Heat transfer analysis in diverging and converging channels, Nonlin. Sci. Lett. A 3 (2012) 61–71.

[21] M. Tatari, M. Dehghan, On the convergence of He's variational iteration method, J. Comp. Appl. Math. 207 (2007) 121–128.